CRYSTAL GROWTH & DESIGN
2004
VOL. 4, NO. 5
905−913

Crystal Growth and Morphology: New Developments in an Integrated Hartman−Perdok−Connected Net−Roughening Transition Theory, Supported by Computer Simulations

P. Bennema,[†,‡] H. Meekes,*[,‡] S. X. M. Boerrigter,[§] H. M. Cuppen,[‡] M. A. Deij,[†,‡] J. van Eupen,[†,‡] P. Verwer,[‡] and E. Vlieg[‡]

Synthon, Microweg 22 Nijmegen, 6545 CM Nijmegen, The Netherlands, NSRIM Laboratory of Solid State Chemistry, University of Nijmegen, Toernooiveld 1, 6525 ED Nijmegen, The Netherlands, and Department of Industrial & Physical Pharmacy, Purdue University, 575 Stadium Mall Drive, West-Lafayette, Indiana 47907-2091

Received September 29, 2003

ABSTRACT: In this paper, 200 years of modeling crystal growth and morphology are reviewed. From the discovery of the law of rational indices, the interplanar distance law of Bravais, Friedel, Donnay, and Harker, to more structural theories such as the Hartman−Perdok theory, as well as statistical mechanical cell models, we arrive at the modern growth theories supported by Monte Carlo growth simulations. Shortcomings in the classical Hartman−Perdok theory are highlighted, and the concept of weakening of connected nets by connected net interactions is explained using a theoretical example. In the last section, our new insights are applied to three examples—crystal structures of venlafaxine, paracetamol, and triacylglycerols—to illustrate their scope and applicability.

1. Introduction

For more than two centuries, people have been trying to relate the macroscopic morphology and the roughening of crystal faces to the microscopic crystal structures. Understanding the crystal morphology is very important and interesting both from a purely scientific point of view and for all kinds of technical applications. In industry, crystals are often formed both as intermediate and end products. Crystallization is often the only viable operation available for purification and isolation. Knowledge of the shape or morphology of these crystals is of crucial importance, since the shape determines many macroscopic properties of the product. Think for instance of the dissolution rate for pharmaceutical compounds, optical properties, solubility, and compressibility but also more process-related characteristics such as rheological characteristics, filtration rate and pressure, agglomeration, etc.

Over the years, separate disciplines have studied the correlation between structure and growth. Recently, these studies were integrated to come to a better understanding of the crystal growth and therefore of the morphology. In this section, we will first explain the mathematical background of crystallography, the BFDH (Bravais, Friedel, Donnay, and Harker) law, the Hartman−Perdok theory, and the statistical mechanical theories of surface roughening transitions, Ising models, and computer simulation models.

Section 2 starts with a theoretical crystal structure to illustrate the effect of weakening of connected nets by multiple connected net interactions. Then, three examples of real compounds are discussed to illustrate the more integrated approach to the modeling of morphology.

* To whom correspondence should be addressed. E-mail: hugom@sci.kun.nl.
† Synthon.
‡ University of Nijmegen.
§ Purdue University.

1.1. Mathematical Backgrounds of Crystallography and Crystal Morphology.

The first important breakthrough in the science of crystallography was the formulation of the law of rational indices.[1,2] This law states that the angles between similar crystallographic faces on different crystals are identical within minutes of arc. Later, it was found that this law is generally applicable to all kinds of inorganic and organic crystals; see for instance the volumes edited by von Groth,[3] who was also the first editor of Zeitschrift für Kristallografie in 1877.

The law of rational indices further describes the orientation of crystallographic faces in reference to a coordinate system. This coordinate system is defined in such a way that it consists of three axes, *A*, *B*, and *C*, taken to be parallel to the three edges of the crystal under investigation. One observed face is taken to be the unit face; it cuts distances *a*, *b*, and *c* from the axes. Now, any observed crystal face will cut pieces a/h, b/k, and c/l from the unit axes, in which h, k, and l (the reciprocal or Miller indices) are taken to be integers including zero, i.e., $h = 0$ implies that the face $(0\ k\ l)$ is parallel to the *A*-axis. The hypothesis that for a three-dimensional (3D) translationally invariant crystal structure a macroscopic face $(h\ k\ l)$ is parallel to a stack of parallel net planes was put forward by Bravais more than a century ago.

After the discovery of rational indices, the current mathematical crystallography was developed in the 19th and the beginning of the 20th century,[1] which is, seen from a modern logical point of view, a branch of Euclidian geometry and mathematical group theory. Nowadays, the resulting 230 space groups, 32 point groups,[4,5] and their implications for the description of 3D crystal structures are summarized in the International Tables for Crystallography.[6]

1.2. Crystals Seen from a Macroscopic and Microscopic Point of View: BFDH Law.

One of the

10.1021/cg034182v CCC: $27.50
Published on Web 07/02/2004

Table 1. Selection Rules of Space Group $P2_1/n$

(h k l)	selection rules, with $n \in Z$
(h 0 l)	$h + l = 2n$
(0 k 0)	$k = 2n$
(h 0 0)	$h = 2n$
(0 0 l)	$l = 2n$

most fascinating aspects of crystals is that due to the crystal growth processes, crystals are generally bound by flat faces. Sometimes, however, crystals are partly or completely bound by rounded faces or have dendritic shapes (for instance, snow crystals). Modern theories of crystal surfaces and crystal growth try to explain under which conditions crystals grow with more or less flat faces (h k l)[7] or with unstable rounded faces, which will develop unstable crystal shapes that change in time.[8−10]

The first successful attempt to predict crystal morphology was the law that nowadays is called the BFDH law, which was developed in the first half of the 20th century. It states that the larger the interplanar distance d_{hkl} for a stack of net planes parallel to a macroscopic plane with orientation (h k l), the lower its growth rate or the higher its morphological importance (MI). Here, the MI of a face (h k l) is a qualitative measure for the relative statistical frequency of occurrence or relative size of a set of symmetry equivalent faces of crystals. The indices (h k l) have to be corrected using the space group selection rules of X-ray crystallography. In Table 1, an example of these rules is given for the space group $P2_1/n$ (the space group of venlafaxine crystals discussed in section 2.2.1). Note that in general the MI of a face is inversely related to its growth rate, i.e., the slowest growing faces dominate the growth morphology of the crystal.

The mathematical BFDH hypothesis seems to work rather well. This can be confirmed by comparing the calculated MI and the resulting pictures of crystal morphologies, with a statistical analysis of the relative sizes of observed crystal faces (h k l).

From a physical, chemical point of view, the relationship between growth rate and d_{hkl} can be rationalized by realizing that the thicker the growth layers d_{hkl} are, the more chemical bonds will have to be formed in the process of creating the growth layer; therefore, the slower the growth rate is. This is especially true if these bonds are isotropic as for simple ionic crystals such as NaCl. For organic molecules, these bonds may be much more anisotropic because in organic crystals the interactions are governed by van der Waals interactions and hydrogen bonding, as well as electrostatic interactions, and these may have large anisotropic contributions, depending on the structure of the molecule.

1.3. Hartman−Perdok Theory. Almost half a century ago, Hartman and Perdok (teachers of P. Bennema) wrote three seminal papers on the morphology of crystals.[11−13] Looking back, they implicitly introduced the concept of what is nowadays called the crystal graph. The Hartman−Perdok theory discerns growth units (GUs) and overall bonds between GUs. The overall bonds between GUs may consist of multiple subbonds, which can be determined computationally using various force fields. The GUs can be molecules, complexes, or ions occurring in the mother phase (melt, solution, or vapor) from which the crystal grows. The crystal graph is therefore a mathematical representation of the crystal structure as an infinite set of translationally invariant vertices and edges, with the same elementary cell and space group as the crystal structure that it represents.

The crystal graph can be used to define periodic bond chains (PBCs), periodic chains of bonds in the crystal graph. Two PBCs in different directions [u v w], which span d_{hkl}, make up a connected net with the crystallographic orientation (h k l). Note that the reciprocal space vector [h k l]* is perpendicular to the corresponding crystal face. Now, we can define F-faces to have a connected net perpendicular to the vector [h k l]*, S-faces to have mutually nonconnected PBCs perpendicular to the vector [h k l]*, and K-faces to have no PBCs perpendicular to [h k l]*.

To try to predict the morphology of crystals, Hartman and Perdok introduced the broken bond energies E^{att}_{hkl} and E^{slice}_{hkl}[11−13] and Hartman and Bennema[14] published a paper in 1980 in which it was shown, by studying theories of crystal growth mechanisms such as spiral growth and two-dimensional (2D) nucleation mechanisms, that relative growth rates of faces (h k l) are in principle proportional to E^{att}_{hkl}. In other words, by calculating the attachment energies of all (h k l), a growth morphology can be predicted.

These concepts above apply to the growth form of crystals but can also be applied to the equilibrium form of a crystal. This form is a—usually very small—crystal, the habit of which is determined by statistical fluctuation processes, rather than growth kinetics. When predicting equilibrium forms, surface tension is considered, and therefore, all attachment energies should be scaled by the mesh area M_{hkl}:

$$E^{\mathrm{att}}_{\mathrm{eq},hkl} = \frac{E^{\mathrm{att}}_{hkl}}{M_{hkl}}$$

This leads to a narrower distribution of $E^{\mathrm{att}}_{\mathrm{eq},hkl}$, resulting in a similar, but richer, morphology as compared to the growth morphology. This is also observed on actual equilibrium forms, which can be produced under very special experimental conditions.[15−17]

1.4. Statistical Mechanical Models. In this section, the occurrence of flat faces (h k l), resulting from the growth process, will be explained in terms of the roughening phase transition, which occurs above the dimensionless critical roughening temperature θ^R, for each crystallographic orientation (h k l).

1.4.1. Roughening Transition of Connected Nets. Connected nets, as defined earlier in the Hartman−Perdok theory, have a nonzero roughening temperature, defined as

$$\theta^R_{hkl} \equiv \left(\frac{2kT}{\Phi^{\mathrm{str}}}\right)_{hkl} \qquad (1)$$

Here, Φ^{str} is the strongest bond in the crystal graph, composed of bonds Φ_1, Φ_2, Φ_3, ..., Φ_i, ... between GUs in the crystal graph. In eq 1, we introduced, according to conventions, a dimensionless temperature θ defined as

$$\theta = \frac{2kT}{\Phi^{\mathrm{str}}} \qquad (2)$$

At the roughening temperature, the edge free energies γ^{uvw} of steps along the direction [*u v w*] coplanar with the crystallographic orientation (*h k l*) becomes equal to zero:

$$\theta < \theta^R_{hkl} \Rightarrow \gamma_{hkl}{}^{uvw} > 0$$

$$\theta \geq \theta^R_{hkl} \Rightarrow \gamma^{uvw}_{hkl} = 0 \qquad (3)$$

When the edge free energy in a certain direction [*u v w*] has become equal to zero, effectively, there is no energy barrier inhibiting growth and the face will grow as a nonfaceted rough face.

The implications for F-, S-, and K-faces are as follows. An F-face is parallel to at least one connected net having two sets of mutually interconnected PBCs in at least two directions [*u v w*]. This means that in all directions [*u v w*], the edge free energy will be larger than zero at a nonzero temperature, and the face will have a roughening transition at $T > 0$. For S-faces, there is only one set of PBCs parallel to a direction [*u v w*] in the face. All other directions [*u v w*] will have a zero edge free energy; therefore, the face will grow as a rough face from $T = 0$. Finally, K-faces are not connected in any direction [*u v w*] and will grow rough from $T = 0$.

1.4.2. Relation between the Ising 2D Spin Order−Disorder Transition and Connected Nets. The Ising 2D spin order−disorder transition is based on a 2D grid of spins, and in the case of simple triangular, hexagonal, or rectangular connected nets, the dimensionless critical Ising temperature, θ^I_{hkl}, can be calculated exactly, provided the ratio of broken bond energies of the 2D nets is known. This temperature roughly marks the transition for a particular connected net, at which its connectedness in terms of free energy is lost. Rijpkema and Knops have developed a formalism in which connected nets of all configurations can be translated to the Ising model.[18] The work of Rijpkema and Knops can be considered to be a generalization of the pioneering work of Onsager,[19] who demonstrated that there is a spin order−disorder phase transition of second order at the critical temperature. Below the transition temperature, two phases exist, one with all spins up, one with all spins down; above the transition temperature, one disordered phase of mixed spins exists. This spin model can be transferred to the crystal growth model by considering solid and fluid (spin up and spin down) phases to occur randomly above the transition temperature (rough growth, edge free energy is equal to zero) and as two separate phases below the roughening temperature (layer-by-layer growth, edge free energy larger than zero).

The theory of Onsager's 2D order−disorder transition served as a basis for the famous seminal paper of Burton, Cabrera, and Frank (BCF).[20] Using a one layer model for the (001) face of the Kossel crystal, they showed that below a critical temperature steps have a finite edge free energy. Below this critical temperature, a crystal surface can grow by a layer mechanism, either by 2D nucleation or by the spiral growth mechanism as proposed by Frank in 1949. Above the critical roughening temperature, a crystal face will grow as a rounded rough face (due to volume diffusion). Nowadays, the crystallographic approach of Hartman and Perdok[11−14] and the statistical mechanical approach of 2D Ising models[18−20] are highly integrated.[7,21]

1.4.3. Survey of Existing Ising Surface Models, Developed and Used Until About 1998. Various statistical mechanical models for crystal surfaces have been studied in the last century. These all use cell models, in which each cell can be either "fluid" or "solid". We will shortly summarize their main features in the list below.

1.4.3.1. The Not Exact Mean Field 2D Model. For instance, the model of Jackson from which it can be derived states that if the well-known α factor ($\alpha = 4\Phi/kT$)[22] of a crystal face (*h k l*) is larger than two this face is growing as a flat face with a layer mechanism (2D nucleation or spiral growth). This implies that below a certain critical, nowadays called roughening temperature, a face (*h k l*) is growing with a layer mechanism as a face with a well-defined orientation (*h k l*) and above this temperature as a rough face in principle without any orientation (*h k l*).

1.4.3.2. The Not Exact Mean Field SOS (Solid on Solid, No Overhangs) 3D Multilayer Mean Field Model. This model was introduced by Temkin,[23] from which it also follows that a critical roughening transition occurs, which marks the transition between "flat" and "rough" growth.

1.4.3.3. The 2D Step Model. This model, in which the SOS condition was introduced by Leamy, Gilmer, and Jackson,[24] can be solved exactly (see also the recent survey paper of Bennema and Meekes[25]).

1.4.3.4. The 2D Cell Models. These models were introduced by BCF and inspired by Onsager and can be solved exactly as well.[19,20] Thanks to Rijpkema and Knops, a generalized version of the Onsager−BCF 2D cell models was introduced, which could be applied to any kind of 2D connected net. It was first applied to the connected nets of the complex garnet structure.[18]

1.4.3.5. Computer Simulations of Growth. In the seventies of the last century, computer simulations to study crystal growth processes were introduced by, among others, Gilmer et al.,[26] using the SOS model introduced by Temkin.[23] (Recall that Temkin used a mean field approach. See also the survey papers[7,21]). It followed from these simulations that for the (001) face of the simple cubic SOS model, above a certain critical value of α, i.e., below the critical roughening temperature, curved growth rates vs driving force curves were obtained, which could be fitted with a birth and spread 2D nucleation model. Below this critical value of α, i.e., above the corresponding critical roughening temperature, a linear rate vs supersaturation curve was obtained. This change from nonlinear 2D nucleation curves to linear curves marked the roughening transition and the roughening temperature.

It can be concluded that considerable progress was made in the field of crystal growth, by applying statistical mechanical models to Ising models of crystal surfaces to study and simulate crystal growth, resulting in an integrated approach to the problem at hand.

2. Recent Developments in Nijmegen

The BFDH law and the attachment energy approach correlate the growth rate of the face to the unit cell and the energies in the crystal structure, respectively, by

making some crude assumptions. In reality, the growth rate is determined by the step free energy, since both birth-and-spread and spiral growth models have this quantity, apart from the supersaturation, as their key parameter. Cuppen et al. have recently published steps toward a generalized theory of crystal growth mechanisms based on this key parameter, the step free energy.[27,28]

Although the step (free) energy determines the growth rate and not the interplanar distance or the attachment energy, both the BFDH and the attachment energy method often give reasonable results for the morphology.[29] This can be explained by considering that large interplanar distances and small attachment energies usually mean large slice energies. For isotropic connected nets, nets in which the bonds are more or less equal in all directions, large slice energies result in large step energies leading to slow growth. An anisotropic connected net consists of a very strong and a very weak PBC; that is, it is connected very strongly in one direction [*u v w*] and very weakly in another direction [*u v w*]′. The two PBCs still make it a connected net, but because of the very weak PBC in one direction, the connected net gets an S-face character and will grow rough.

Another effect that can cause an increase in the growth rate of the surface with respect to the expected growth rate from the attachment energy is weakening due to multiple connected net interactions, as will be explained by the following example.

2.1. Multiple Connected Net Interactions. About five years ago, the physical implications for crystal growth mechanisms and crystal morphology of the occurrence of two or more alternative connected nets for one orientation (*h k l*) became apparent.[30−32] Before this discovery, we simply selected the strongest connected net out of a stack of alternative connected nets, which corresponded to the highest E^{slice} or highest Ising temperature for the orientation (*h k l*) under consideration. It was simply assumed that this strongest connected net would dominate the crystal growth process.

Detailed investigation, however, revealed that when a potential nucleus is formed on a connected net, differential bonds come into play if there are multiple connected nets. As a result, a substitute net can be formed to account for the appearance of these differential bonds. The substitute net can be considerably weaker than the original nets present in the structure.

To demonstrate the phenomenon, we present a simple model crystal graph seen in the [100] direction (see Figure 1). In this direction, perpendicular to the plane of the paper, equally strong bonds are present, which have the same length as the unit of length of the *a*-axis. They form one set of PBCs, which is used to complement all connected nets.

It can be seen from Figure 1 that the crystal graph can be partitioned in connected nets (011) and ($0\bar{1}1$) consisting of the PBCs [$0\bar{1}1$] and [011], respectively, and the PBC [100]. The PBC [$0\bar{1}1$] consists of the bonds a_1 and b_2 (with bond energies Φ_{a1} and Φ_{b2}) and the PBC [011] consists of the bonds a_2 and b_1, respectively (corresponding with bond energies Φ_{a2} and Φ_{b1}). There are no other connected nets in these orientations; therefore, they are singlets. The edge energy of the (011) net is either Φ_{b1} or Φ_{a2}, and for the ($0\bar{1}1$) net, the edge energies are either Φ_{a1} or Φ_{b2}.

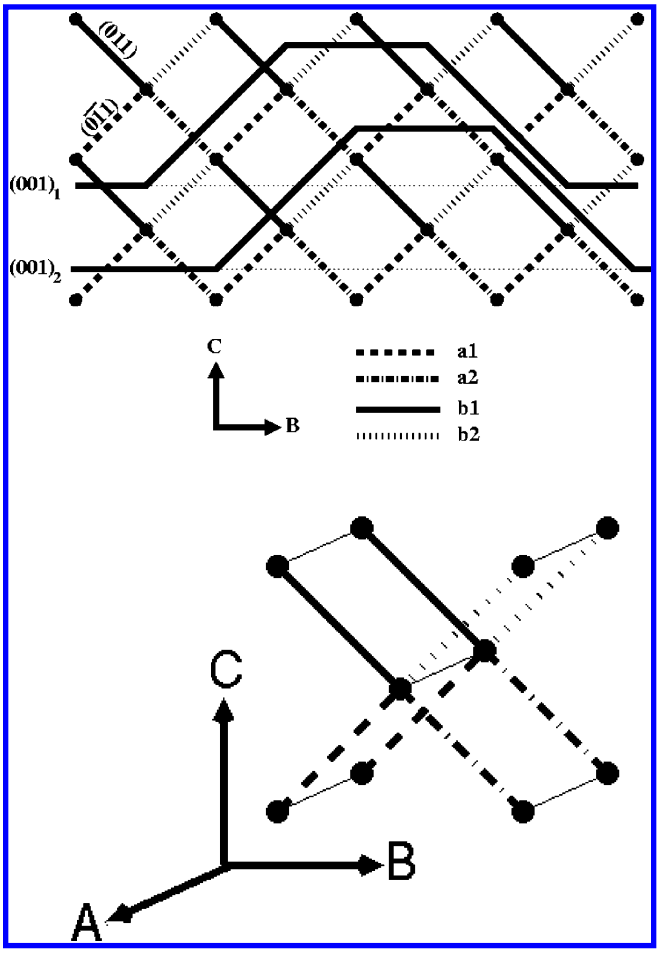

Figure 1. Model graph for illustration of weakening by multiple connected net interactions is shown here. The bonds in the direction of the *a*-axis are only shown in the lower 3D picture of the graph. These bonds make the model graph connected and are present perpendicular to the paper in the upper figure.

It can be seen from Figure 1 that there are two parallel connected nets in the (001) direction, $(001)_1$ and $(001)_2$, made up of a_1 and a_2 and b_1 and b_2, respectively. In the calculation of the edge energies ϵ_1 and ϵ_2 of these nets, we encounter the difference bonds. This can be viewed as follows: when we make the edge of net $(001)_1$, we cut the bonds b_1 and b_2, but at the same time, because we make the edge, we prevent the breaking of bonds a_1 and a_2. The net energy difference ϵ_1 is therefore $(\Phi_{a1} - \Phi_{b1}) + (\Phi_{a2} - \Phi_{b2})$. Similarly, if we make the edge for net $(001)_2$, we cut bonds a_1 and a_2, but bonds b_1 and b_2 are formed, making the net energy difference ϵ_2 equal to $(\Phi_{b1} - \Phi_{a1}) + (\Phi_{b2} - \Phi_{a2})$.

Now, depending on the magnitudes of all Φs, either ϵ_1 or ϵ_2 is negative. In the case that ϵ_1 is negative, the crystal will grow with layers shaped like connected net $(001)_2$, or when ϵ_2 is negative, it will grow with layers shaped like $(001)_1$. There is a special third case, when $\Phi_{a1} = \Phi_{b1}$ and $\Phi_{a2} = \Phi_{b2}$ or if $(\Phi_{b1} - \Phi_{a1}) = -(\Phi_{b2} - \Phi_{a2})$. Then, both ϵ_1 and ϵ_2 are equal to zero, and the face will have zero edge free; therefore, it will have zero edge free energy for both nets. Effectively, the face becomes an S-face, and the face will grow rough already at $T =$

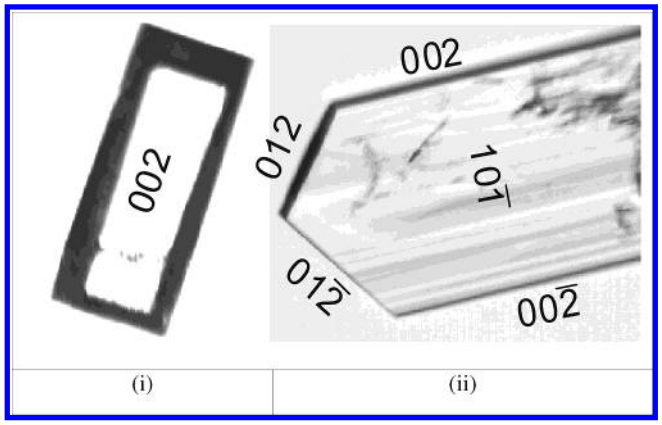

Figure 2. Experimentally observed morphologies of the free base form of venlafaxine. (i) Top view: Front and back face {002}; side faces {10$\bar{2}$}; and top and bottom faces {012}. (ii) Detailed side view of the {012} top/bottom faces.

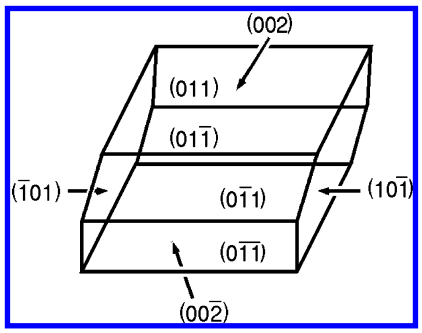

Figure 3. Morphology of the free base form of venlafaxine predicted by the attachment energy method. The {001} and {10$\bar{1}$} orientations are predicted correctly.

0; we called this rather exceptional situation a case of symmetry roughening.

Another interesting case occurs when one of the bonds Φ_i ($i = a_1$, a_2, b_1, or b_2) has zero bond strength. Take for example $\Phi_{a1} = 0$. The connected net $(001)_1$ is no longer connected, and the connected net $(001)_2$ becomes the only connected net in the (001) orientation. When calculating the edge energy ϵ, the result is $\Phi_{b1} + (\Phi_{b2} - \Phi_{a2})$. So, even though there is only a single connected net (i.e., a singlet), the edge energy is still lower than expected from the attachment energies, because of difference bonds. The latter situation was found for the first time for fat crystals, which will be discussed further on in section 2.2.3.

The result for the morphology of the present example is that depending on the exact magnitude of the bonds, the (001) faces grow relatively fast and may or may not appear on the morphology. This is due to the occurrence of difference bonds, as 2D nucleation and roughening barriers of the (001) faces may be reduced considerably, as compared to the nucleation and roughening barriers for the orientations (011) and (0$\bar{1}$1). Because of this gradual reduction, a sharp distinction between F- and S-faces seems to become more of a gliding scale, depending not only on the magnitude of individual bonds but also on the topology of the bonds in the surface of an orientation (*h k l*).

Recently, many more examples of crystal structures for which difference bonds determine the growth rate of orientations (*h k l*) were found. If the topology of a

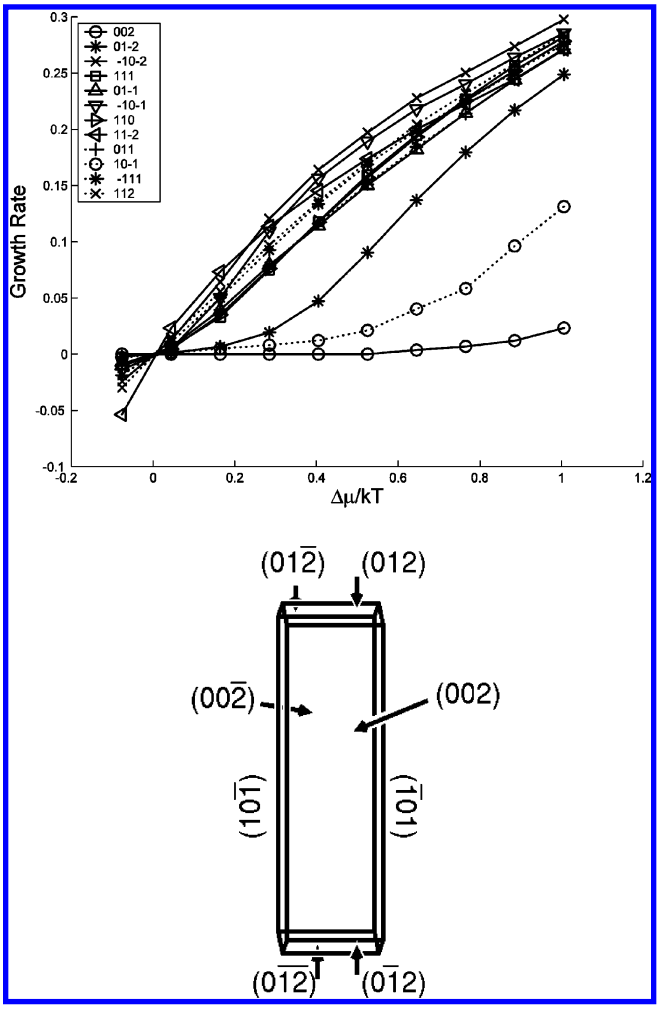

Figure 4. In this figure, the growth rate vs supersaturation curves are shown, from the Monte Carlo calculations on various crystallographic orientations of the crystal graph of venlafaxine free base. Below, the resulting morphology is shown for $\Delta\mu/kT = 0.89$. The morphology is corresponding very well with the one observed experimentally (see Figure 2).

stack of connected nets with orientation (*h k l*) becomes very complex, we may give up carrying out a topological analysis and simply carry out a Monte Carlo growth simulation, which will provide us with a growth rate vs supersaturation curve of this orientation. For this, the program MONTY was developed. MONTY can run a Monte Carlo simulation of growth for any orientation of any crystal structure, based on information from the crystal graph.

The Monte Carlo simulations are based on an "atomistic" lattice growth simulation, in which the "atoms" or GUs represent the molecules that can grow or etch from fixed lattice points. The program has a flexible probability scheme, which we can use to simulate either growth or etching conditions. As the program does not consider surface diffusion, it is particularly suited for solution growth, for which it is known that the surface diffusion is much lower, as compared to growth from the gas phase. We have learned from various recent Monte Carlo studies that despite the assumptions described above, the MONTY growth simulations are susceptible to the subtle implications of the bonding topology of an orientation (*h k l*) of a certain crystal graph.[33–35]

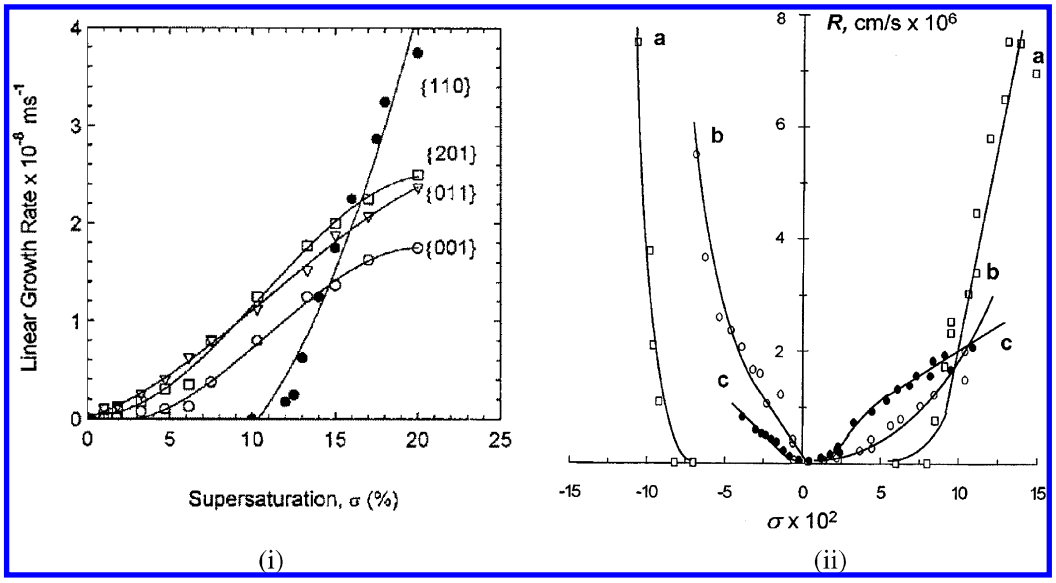

Figure 5. Growth rate vs supersaturation curves of paracetamol grown from aqueous solution as measured by (i) Ristic et al. and (ii) Shekunov. Curve *a* represents growth and dissolution of {110}, curve *b* represents growth and dissolution of {20$\bar{1}$}, and curve *c* represents growth and dissolution of {001}.

2.2. Examples. 2.2.1. Venlafaxine Free Base. In collaboration with the pharmaceutical company Synthon B. V., we recently applied both the Hartman−Perdok theory and the Monte Carlo growth simulations mentioned above to the problem of predicting the morphology of the free base form of venlafaxine: (*N*,*N*-dimethyl)-2-(1-hydroxycyclohex-1-yl)-2-(4-methoxyphenyl)ethylamine.[36] The experimental morphology has MI {002} > {10$\bar{1}$} > {012} and is shown in Figure 2.

From the connected net analysis, we find that two of the three observed faces, {012} and {10$\bar{1}$}, are singlet connected nets. The third face, {002}, is not a singlet face, but the two strongest connected nets of the {002} orientation are not able to weaken each other as they do not share any bonds or GUs. All other crystallographic orientations have multiple connected nets that do share bonds, and these orientations are not observed in the experimental morphology. In short, only the orientations that do not suffer from the weakening of nets due to differential bonds or orientations that have only one unique connected net are observed in the morphology.

The morphology predicted from attachment energies is shown in Figure 3. It can be seen that although the three connected nets are observed in the experimental morphology, the {012} orientation is not predicted. Instead, we see the {011}, as its attachment energy is a little bit lower than the attachment energy of {012}. The attachment energy approach also does not correctly predict the rectangular morphology of the {002} face; instead, it predicts an almost square morphology.

From the Monte Carlo simulations, done at relative supersaturations $\Delta\mu/kT$ approximately between 0 and 1, the findings of the Hartman−Perdok theory are corroborated as follows: the slowest growing faces are the faces with only one connected net. In the case of these growth simulations, however, the {012} face grows slower than the {011} face; therefore, it dominates the morphology. Also, the rectangular form of the {002} face is predicted correctly. The predicted morphology and the growth rate, dependent on the relative supersaturation, are shown in Figure 4.

2.2.2. Paracetamol. Many studies have been devoted to the crystal growth behavior of paracetamol (acetaminophen). All of these studies show that the growth morphologies of paracetamol strongly depend on the driving force for crystallization and are mainly determined by the {001}, {011}, {110}, and {20$\bar{1}$} faces. Studies of the surface topology of these faces show that the spirals on the {110} face are not active and this face grows via 2D nucleation. The other two faces grow via spiral growth. Figure 5a,b shows the experimental growth rate curves for some of the faces as measured by Ristic and Sherwood and co-workers[37] and by Shekunov.[38] Both panels show a gradual increase in growth rate for the spiral growth faces and a dead zone followed by a rapid increase of growth rate for the {110} faces. There is, however, some discrepancy between the two plots about the order of the {20$\bar{1}$} and the {001} faces.

The strong supersaturation dependence of the morphology of paracetamol is mainly due to the growth behavior of the {110} face. This growth behavior cannot be explained based on the attachment energy method or the BFDH law, since both methods do not include temperature, growth mechanism, or supersaturation. With Monte Carlo simulations, these parameters can be introduced. Another advantage of this method is that different growth mechanisms—2D nucleation and spiral growth—can be included. We have performed Monte Carlo simulations for the four major faces and have determined the growth rate as a function of the driving force for crystallization. For the {110} face, only the 2D nucleation mechanism is used; for the other faces, a combination of spiral growth and 2D nucleation is used. The results are shown in Figure 6. As can be seen in this figure, the three faces with a spiral growth mechanism show a gradual increase in growth rate. The {110} face on the other hand has a nucleation barrier and then a rapid increase, crossing all other curves. The supersaturation dependence of the morphology can

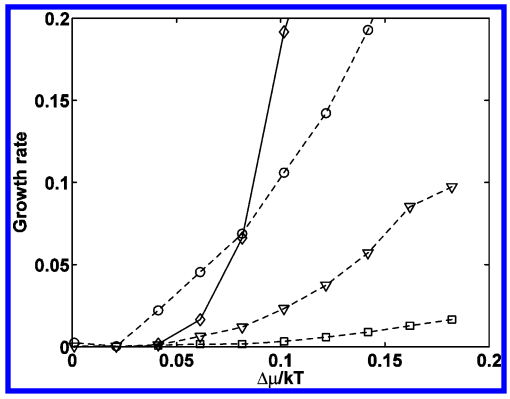

Figure 6. Growth rates vs driving force of crystallization as measured by the Monte Carlo simulations. The {20$\bar{1}$}, {011}, and {001} faces (dashed lines) have screw dislocations. The {110} face (solid line) grows via the 2D nucleation mechanism.

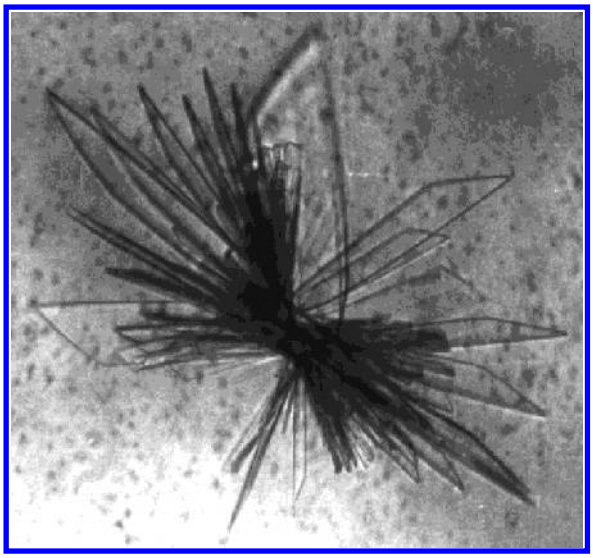

Figure 7. 16.16.16-Triacylglycerol crystals growing from a spherulite at high supersaturation. The planklike habit can be observed as larger fragments sticking out from the core of the spherulite.

therefore be explained by the difference in growth mechanism.

2.2.3. Morphology of Three Types of Fat Crystals. In the following, we will very briefly mention results of the application of the theory to explain the morphology of three types of fat crystals.

2.2.3.1. Morphology of Crystals of *β*-n.n.n-Triacylglycerol. In 1992, a paper was published by Bennema, Vogels, and de Jong[39] in which an explanation was given on the basis of attachment energies for the morphology of the centrosymmetric *β*-*n.n.n*-triacylglycerol crystals (corresponding to one of the three known different fat crystal structures consisting of fat molecules with three paraffin chains each with *n* carbon atoms). It was derived from the theory that the MI of the dominant faces parallel to the *b*-axis would be {001} ≫ {100} > {101}. This ratio of MI will give these crystals (independent of the solvent) a planklike habit (see Figure 7). The direction of elongation is parallel to the *b*-axis.

It followed, however, from the paper of 1992 that for the top faces of the observed planklike crystals a serious discrepancy between the attachment energy morphology

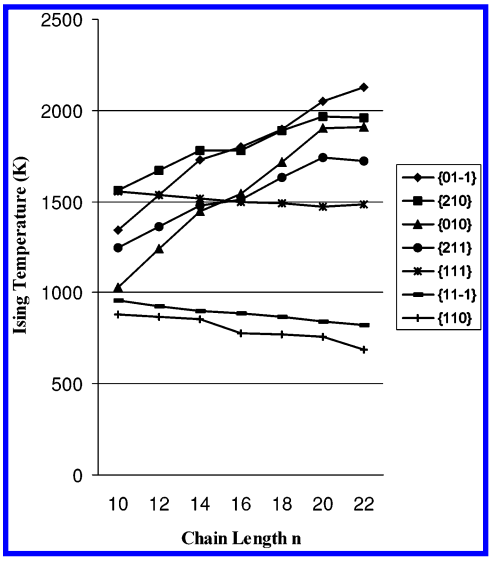

Figure 8. Relative Ising temperatures for the top faces of *β*-*n.n.n* fat crystals as a function of the chain length *n*.

and the experimental morphology was observed. In the paper of 1992, we assumed that the strongest connected net out of the 32 connected nets, corresponding to alternative top faces not parallel to the *b*-axis, would have the highest edge (free) energies and would have the lowest growth rate and hence the highest MI.

Once the difference bonds were taken into account, the morphology of the top faces of the fat crystal turned out to be in perfect agreement with the observed top faces of the growth forms. Moreover, the morphology of the fast growing top faces of these fat crystals was explained for different carbon chain lengths from 10 to 22 carbon atoms.[35] Figure 8 shows the calculated relative Ising temperatures as an estimate of the relative roughening temperatures for the top faces of these fat crystals as a function of the chain length *n*.

For these calculations, the step energies on these top faces were determined by considering the difference bonds mentioned above. The higher the roughening temperature of a face (*hkl*), the lower its growth rate and, therefore, the higher its MI. In Figure 9, the experimental top faces are presented for *β*-10.10.10 and *β*-16.16.16 showing that the (01*l*) top faces are present for both fat crystals but that the (11*l*) faces present for *β*-10.10.10 are replaced by (21*l*) faces for *β*-16.16.16. In Figure 8, one observes the same order of MI as a result of the strong difference in chain length dependence of the Ising temperatures for the {111} and {210}.

In more recent publications, these results were compared to the morphology of two other fat crystal structures, namely, those of the *β*′-10.12.10 and the *β*′-16.16.14 crystals.[40] The former forms even more elongated thin needles while the latter has relatively slowly growing top faces resulting in lozenge-shaped crystals. In all cases, the attachment energy method correctly predicts thin crystals with relatively large (001) faces. The aspect ratio of the side faces as compared to the top faces, however, is predicted badly. A detailed study of the bonding topology of the top faces as compared to the side faces led to an explanation for these rather extreme differences in morphology for these three fat crystal structures. These studies were supported by Monte Carlo simulations.[34]

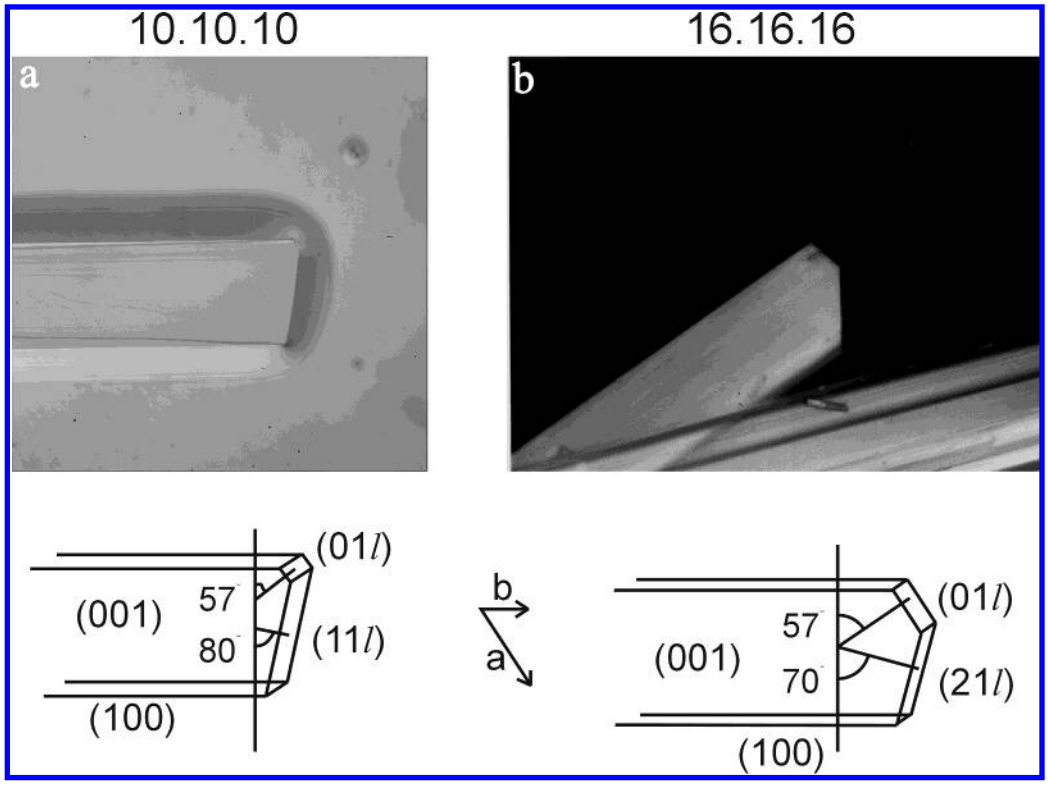

Figure 9. Experimental top faces for β-10.10.10 and β-16.16.16 fat crystals. The indices l are difficult to determine because of the thinness of the crystals.

3. Summary and Conclusions

In this paper, we have shown that the old science of crystal morphology prediction is still evolving. Morphology predictions such as the BFDH and attachment energy methods have been used for years with varying success, and discrepancies between model and experiment were often attributed to effects of solvent or unwanted impurities. Alternatively, some of these discrepancies could be explained by the fact that the methods mentioned above do not cover parameters such as temperature, supersaturation, and growth mechanism. Temperature mainly shows up in roughening of crystal faces, usually resulting in relatively high growth rates depending on the growth orientation (h k l). Supersaturation and growth mechanism dependencies lead to a change in relative growth rates of the various faces of a crystal, frequently observed. All of these three parameters are intimately related to the edge free energy of steps on crystal surfaces. During the last five years, it was realized that the edge free energy of a crystal face is not always, and in fact quite often not, simply determined by the slice energy of the corresponding growth slice. Therefore, detailed studies of the edge free energies are essential to understand crystal growth behavior. For that study, we have shown that the crystal graph is an essential tool. Real crystals usually have rather complicated crystal graphs. Then, Monte Carlo simulations on real crystals provide a valuable tool to study the growth behavior. To understand the results of these simulations, the existing crystal growth theories, which are almost always based on very simple crystal models, have to be generalized to crystal growth mechanisms on real crystals. Some first steps in this direction have recently been realized.[27,28] One of the essential tools to apply such generalized crystal growth theories to real crystals will be one that allows for the automated determination of crystal growth steps on any face for a given crystal structure. The latter will be possible using a program called STEPLIFT, currently under development.[41]

References

(1) Burke, J. G. *Origins of the Science of Crystals*; University of California Press: Berkeley, 1966.
(2) Hooykaas, R. *Geschiedenis der Natuurwetenschappen* (in Dutch); Oosthoek Uitgeversmaatschappij NV: Utrecht, 1971.
(3) von Groth, P. *Chemische Kristallografie*; Wilh. Engelmann-Verlag: Leipzig, 1906−1920.
(4) Buerger, M. J. *Elementary Crystallography*; John Wiley & Sons: New York/London, 1963.
(5) Janssen, T. *Crystallographic Groups*; North-Holland/American Elsevier: New York, 1973.
(6) *International Tables for X-ray Crystallography*; Kluwer Academic Publishers: Dordrecht/Boston/London, 1996.
(7) Bennema, P. In *Handbook of Crystal Growth*; Hurle, D. T. J., Ed.; Elsevier: Amsterdam, 1993; Vol. 1a, Fundamentals: Thermodynamics and Kinetics, pp 477−581.
(8) Sekerka, R. F. In *Crystal Growth: An Introduction*; Hartman, P., Ed.; North-Holland/American Elsevier: Amsterdam, London, 1973; Vol. 1, pp 403−443.
(9) Billia, B.; Trivedi, R. In *Handbook of Crystal Growth*; Hurle, D. T. J., Ed.; North-Holland: Amsteram, London, 1993; Vol. 1b, Fundamentals: Transport and Stability, pp 899−1074.
(10) Glicksman, M. E.; Marsh, S. P. In *Handbook of Crystal Growth*; Hurle, D. T. J., Ed.; North-Holland: Amsterdam, London, 1993; Vol. 1b, Fundamentals: Transport and Stability, pp 1075−1122.
(11) Hartman, P.; Perdok, W. G. *Acta Crystallogr.* **1955**, *8*, 525−529.
(12) Hartman, P.; Perdok, W. G. *Acta Crystallogr.* **1955**, *8*, 521−524.
(13) Hartman, P.; Perdok, W. G. *Acta Crystallogr.* **1955**, *8*, 49−52.
(14) Hartman, P.; Bennema, P. *J. Cryst. Growth* **1980**, *49*, 145−156.

(15) Kern, R. In *Morphology of Crystals*; Sunagawa, I., Ed.; Terra Scientific Publishing Company: Tokyo, 1987; Vol. A, pp 77−206.
(16) Toschev, S. In *Crystal Growth: An Introduction*; Hartman, P., Ed.; North-Holland/American Elsevier: Amsterdam, London, 1973; Vol. 1, pp 328−341.
(17) Bennema, P. In *Crystal Growth: An Introduction*; Hartman, P., Ed.; North-Holland/American Elsevier: Amsterdam, London, 1973; Vol. 1, pp 342−357.
(18) Rijpkema, J. J. M.; Knops, H. J. F.; Bennema, P.; van der Eerden, J. P. *J. Cryst. Growth* **1982**, *61*, 295−306.
(19) Onsager, L. *Phys. Rev.* **1944**, *65*, 117−149.
(20) Burton, W. K.; Cabrera, N.; Frank, F. C. *Philos. Trans. R. Soc. London A* **1951**, *243*, 299−358.
(21) Bennema, P.; van der Eerden, J. P. In *Morphology of Crystals*; Sunagawa, I., Ed.; Terra Scientific Publishing Company: Tokyo, 1987; Vol. A, pp 1−75.
(22) Jackson, K. A. *Liq. Metals Solidification* **1958**, 174−186.
(23) Temkin, D. E. In *Crystallization Processes*; Sirota, N. N., Gorskii, F. K., Varikash, V. M., Eds.; Consultants Bureau: New York, 1966; pp 15−22.
(24) Leamy, H. J.; Gilmer, G. H. *J. Cryst. Growth* **1974**, *24/25*, 499−502.
(25) Bennema, P.; Meekes, H. In *Nanoscale Structure and Assembly at Solid−Fluid Interfaces*; Liu, X. Y., De Yoreo, J., Eds. Kluwer Academic Publisher: Boston, 2004; In press.
(26) Gilmer, G. H.; Bennema, P. *J. Appl. Phys.* **1972**, *43*, 1347−1360.
(27) Cuppen, H. M.; Meekes, H.; van Enckevort, W. J. P.; Bennema, P.; Vlieg, E. *Surf. Sci.* **2003**, *525*, 1−12.
(28) Cuppen, H. M.; Meekes, H.; van Veenendaal, E.; van Enckevort, W. J. P.; Bennema, P.; Reedijk, M. F.; Arsic, J.; Vlieg, E. *Surf. Sci.* **2002**, *506*, 183−195.
(29) Docherty, R.; Clydesdale, G.; Roberts, K. J.; Bennema, P. *J. Phys. D: Appl. Phys.* **1991**, *24*, 89−99.
(30) Grimbergen, R. F. P.; Meekes, H.; Bennema, P.; Strom, C. S.; Vogels, L. J. P. *Acta Crystallogr. A* **1998**, *54*, 491−500.
(31) Meekes, H.; Bennema, P.; Grimbergen, R. F. P. *Acta Crystallogr. A* **1998**, *54*, 501−510.
(32) Grimbergen, R. F. P.; Meekes, H.; Bennema, P. *Acta Crystallogr. A* **1999**, *55*, 84−94.
(33) Sweegers, C.; Boerrigter, S. X. M.; Grimbergen, R. F. P.; Meekes, H.; Fleming, S.; Hiralal, I. D. K.; Rijkeboer, A. *J. Phys. Chem. B* **2002**, *106*, 1004−1012.
(34) Boerrigter, S. X. M.; Josten, G. P. H.; van de Streek, J.; Hollander, F. F. A.; Los, J.; Bennema, P.; Meekes, H. *J. Phys. Chem. B*, In press. Information on MONTY: hugom@sci.kun.nl.
(35) (a) Hollander, F. F. A.; Boerrigter, S. X. M.; van de Streek, J.; Grimbergen, R. F. P.; Meekes, H.; Bennema, P. *J. Phys. Chem. B* **1999**, *103*, 8301−8309; ibid. (b) Bennema, P.; Hollander, F. F. A.; Boerrigter, S. X. M.; Grimbergen, R. F. P.; van de Streek, J.; Meekes, H. In *Crystallization Processes in Fats and Lipid Systems*; Garti, N., Sato, K., Eds.; Marcel Dekker Inc.: New York, 2001; pp 105−150.
(36) Deij, M. A.; van Eupen, J.; Meekes, H.; Verwer, P.; Bennema, P.; Vlieg, E. To be published.
(37) Ristic, R. I.; Finnie, S.; Sheen, D. B.; Sherwood, J. N. *J. Phys. Chem. B* **2001**, *105*, 9057−9066.
(38) Shekunov, B. Y.; Grant, D. J. W. *J. Phys. Chem. B* **1997**, *101*, 3973−3979.
(39) Bennema, P.; Vogels, L. J. P.; de Jong, S. *J. Cryst. Growth* **1992**, *123*, 141−162.
(40) Hollander, F. F. A.; Boerrigter, S. X. M.; van de Streek, J.; Bennema, P.; Meekes, H.; Yano, J.; Sato, K. *J. Phys. Chem. B* **2003**, *107*, 5680−5689.
(41) Deij, M. A.; Meekes, H.; Verwer, P.; Vlieg, E. To be published.

CG034182V